Pathiraja, S.; Westra, Seth Pieter; Sharma, Ashish
Why continuous simulation? The role of antecedent moisture in design flood estimation
Water Resources Research, 2012; 48:W06534

Why continuous simulation? The role of antecedent moisture in design flood estimation

S. Pathiraja,[1] S. Westra,[2] and A. Sharma[1]

Received 1 June 2011; revised 28 April 2012; accepted 17 May 2012; published 27 June 2012.

[1] Continuous simulation for design flood estimation is increasingly becoming a viable alternative to traditional event-based methods. The advantage of continuous simulation approaches is that the catchment moisture state prior to the flood-producing rainfall event is implicitly incorporated within the modeling framework, provided the model has been calibrated and validated to produce reasonable simulations. This contrasts with event-based models in which both information about the expected sequence of rainfall and evaporation preceding the flood-producing rainfall event, as well as catchment storage and infiltration properties, are commonly pooled together into a single set of "loss" parameters which require adjustment through the process of calibration. To identify the importance of accounting for antecedent moisture in flood modeling, this paper uses a continuous rainfall-runoff model calibrated to 45 catchments in the Murray-Darling Basin in Australia. Flood peaks derived using the historical daily rainfall record are compared with those derived using resampled daily rainfall, for which the sequencing of wet and dry days preceding the heavy rainfall event is removed. The analysis shows that there is a consistent underestimation of the design flood events when antecedent moisture is not properly simulated, which can be as much as 30% when only 1 or 2 days of antecedent rainfall are considered, compared to 5% when this is extended to 60 days of prior rainfall. These results show that, in general, it is necessary to consider both short-term memory in rainfall associated with synoptic scale dependence, as well as longer-term memory at seasonal or longer time scale variability in order to obtain accurate design flood estimates.

Citation: Pathiraja, S., S. Westra, and A. Sharma (2012), Why continuous simulation? The role of antecedent moisture in design flood estimation, *Water Resour. Res.*, *48*, W06534, doi:10.1029/2011WR010997.

1. Introduction

[2] Flood estimation is arguably one of the most important tasks in engineering hydrology, and constitutes a necessary element for a diversity of planning and engineering design decisions, ranging from the zoning of new land in and around floodplains, through to the design and management of infrastructure such as storm water systems, roads and bridges, flood protection works, and reservoirs. In many cases such decisions are made using a design flood value, which is defined as a hypothetical flood event—usually measured in terms of a single attribute such as its peak flow, level, volume, or response time—which will be equaled or exceeded with a given frequency [*Pilgrim and Cordery*, 1993]. The use of a design flood, as opposed to an observed (historical) event, can then feed into a risk-based decision making framework, in which the likelihood that a flood of given magnitude will occur can be considered alongside the expected consequences of such an event. This can then provide a sound basis for optimally allocating the investment required to manage such floods.

[3] There are a number of alternatives available for the estimation of a design flood, ranging from a frequency analysis of observed streamflow data through to the use of rainfall-runoff models using generated continuous rainfall sequences or a specified design storm [*Beven*, 2002; *Boughton and Droop*, 2003]. Probably the most common class of methods in-use today take as their starting point the estimation of a design rainfall event, which is then translated to a design runoff value of the same exceedance probability through the use of a rainfall-runoff model. The features of this class of methods include: (1) the availability of long historical rainfall records, which at least in the preanthropogenic climate change period can be assumed to be approximately stationary (although see *Ropelewski and Halpert* [1987] for a discussion on the influence of natural variability); (2) the widespread translation of this historical data into design rainfall estimates, typically referred to as intensity-frequency-duration (IFD) relationships, which are often presented as spatial maps in guidance documents such as Australian Rainfall and Runoff [*Pilgrim*, 1987] or the United States National Oceanic and Atmospheric

[1]School of Civil and Environmental Engineering, University of New South Wales, Sydney, NSW, Australia.
[2]School of Civil, Environmental and Mining Engineering, University of Adelaide, Adelaide, SA, Australia.

Corresponding author: S. Westra, School of Civil, Environmental and Mining Engineering, University of Adelaide, Adelaide, SA 5008, Australia. (swestra@civeng.adelaide.edu.au)

0043-1397/12/2011WR010997

Administration (NOAA) Atlas 14, and thus can be used even in locations where gauged records are unavailable; and (3) the diversity of well-established methods for translating design rainfall to design runoff, ranging from simple models such as the rational method [*Kuichling*, 1889; *Mulvaney*, 1851] which translates the design rainfall to a design flow rate, through to more complex event-based rainfall-runoff models which seek to capture various physical processes involved in the transformation from rainfall to runoff and often can be used to estimate the complete flood hydrograph.

[4] An important objective of any rainfall-runoff model used for the purposes of design flood estimation is therefore the maintenance of exceedance probability neutrality between rainfall and runoff, such that by inputting design rainfall of a given exceedance probability, it is possible to obtain the design runoff value of the same exceedance probability [*Kuczera et al.*, 2006]. Given the complexity of the physical processes involved in translating rainfall to runoff, achievement of exceedance probability neutrality invariably requires the adjustment of model parameters through the process of calibration, in which the parameters of a rainfall-runoff model are optimized such that the modeled hydrographs match a set of observed hydrographs as closely as possible over the set of calibration events [e.g., see *Beven*, 2002]. It should be noted that this applies equally in gauged and ungauged catchments, with calibration in ungauged basins usually taking place using data from nearby locations or from catchments with "similar" physiographic characteristics [*Bloschl*, 2005]. As a result of this calibration step, a large range of both physiographic catchment features and climate features become implicitly embedded within the model parameters, including the expected value of antecedent catchment moisture content [*Bloschl*, 2005], with this latter feature having a significant bearing on catchment infiltration properties and the fraction of rainfall which makes its way into the flood hydrograph.

[5] Understanding the role of antecedent conditions on runoff therefore represents an important consideration in flood modeling, particularly in arid areas in which there is a large difference in terms of catchment discharge properties between dry and wet periods, as well as for catchments with large storages such as those with large reservoirs or multiple smaller on-farm dams or storm water detention basins. To illustrate this issue, consider catchment 401210, a small (407 km^2) catchment located in the southeast of Australia, with a mean annual rainfall value of 1212 mm and a coefficient of variation of 2.4 (see Figure 1). This is an unregulated catchment which has not undergone significant changes over the period of record, such that changes in runoff behavior over time can be largely attributed to the influence of atmospheric processes (notably rainfall and evapotranspiration) acting on the catchment. In reviewing the historical record for this catchment, it can be seen that two very similar peak rainfall events lead to markedly different peak runoff events (Figures 2a and 2b), with the distinguishing feature between these two events being the rainfall falling in the days prior to the "flood producing" rainfall event. If the model parameters were calibrated to only one of these events without explicitly considering the antecedent rainfall, there will be a high likelihood that the model parameters will not yield outputs which are exceedance-probability neutral across the full range of events. This is of particular concern when extrapolating to much rarer floods, as the expected value of the antecedent moisture might not be the same for smaller floods (that are typically used for model calibration) as they would be for larger floods (that are often of most interest for design purposes). To add to this issue, a recent study by *Pui et al.* [2011] using data from eastern Australia found evidence of interdecadal variability in the antecedent rainfall preceding the flood producing rain event, this variability being the primary cause of variability in the estimated design flood values. Other climatic influences on soil moisture memory have also been noted by several researchers, for instance, the variation of soil moisture memory with seasonality of the atmospheric state [*Douville et al.*, 2007; *Koster and Suarez*, 2001], as well as the tendency for soil moisture memory to extend for longer time periods in drier climates than warm wet climates [*Wu and Dickinson*, 2004]. Consequently, the issue of the relationship between antecedent moisture conditions and the intensity of the flood-producing rainfall event is becoming of increasing interest in the context of anthropogenic climate change [e.g., *Cameron et al.*, 2000], as mean annual rainfall and evaporation, which in combination have a significant influence on antecedent catchment wetness, are not expected to change by the same magnitude or even in the same direction as the extreme flood-producing rainfall events in most parts of the world [*Bates et al.*, 2008].

[6] Some effort has been placed in explicitly modeling antecedent moisture in the event-based rainfall-runoff modeling process. For example, initial loss parameters in certain models might be linked to an antecedent precipitation index (API) [*Cordery*, 1970], which is made up of a weighted sum of the rainfall in the hours and days leading up to the event, with greater weighting for rainfall immediately preceding the design rainfall event. An alternative approach involves embedding the design rainfall event of duration equal to the time of concentration within a longer duration design storm [*Rigby and Bannigan*, 1996; *Rosso and Rigby*, 2006]. In both these cases, determining the appropriate period for which antecedent precipitation should be explicitly factored into the rainfall-runoff model is difficult. For example, it is common to assume a period of only 5–14 days prior to the design rainfall event for the API [*Heggen*, 2001], which is generally regarded as sufficient to capture synoptic-scale dependence of rainfall [*Van den Dool*, 2007]. However, in the case of the example catchment described above, it can be seen that the magnitude of the flood-producing rainfall for two events shown in Figures 2c and 2d are very different, even though both the runoff response, and the antecedent rainfall in the week prior to the event are very similar. In fact, a frequency analysis on the rainfall show that the daily rainfall for this day was equivalent to the 1% AEP and 50% AEP storm for Figures 2c and 2d, respectively, whereas the runoff for both events had an annual exceedance probability of approximately 60%. The primary difference between these two events was found in the rainfall in the month prior to the event (but not including the week immediately prior), in which the rainfall is well under half for Figure 2c compared with Figure 2d. Although the results in this figure do not provide conclusive evidence of the importance of antecedent

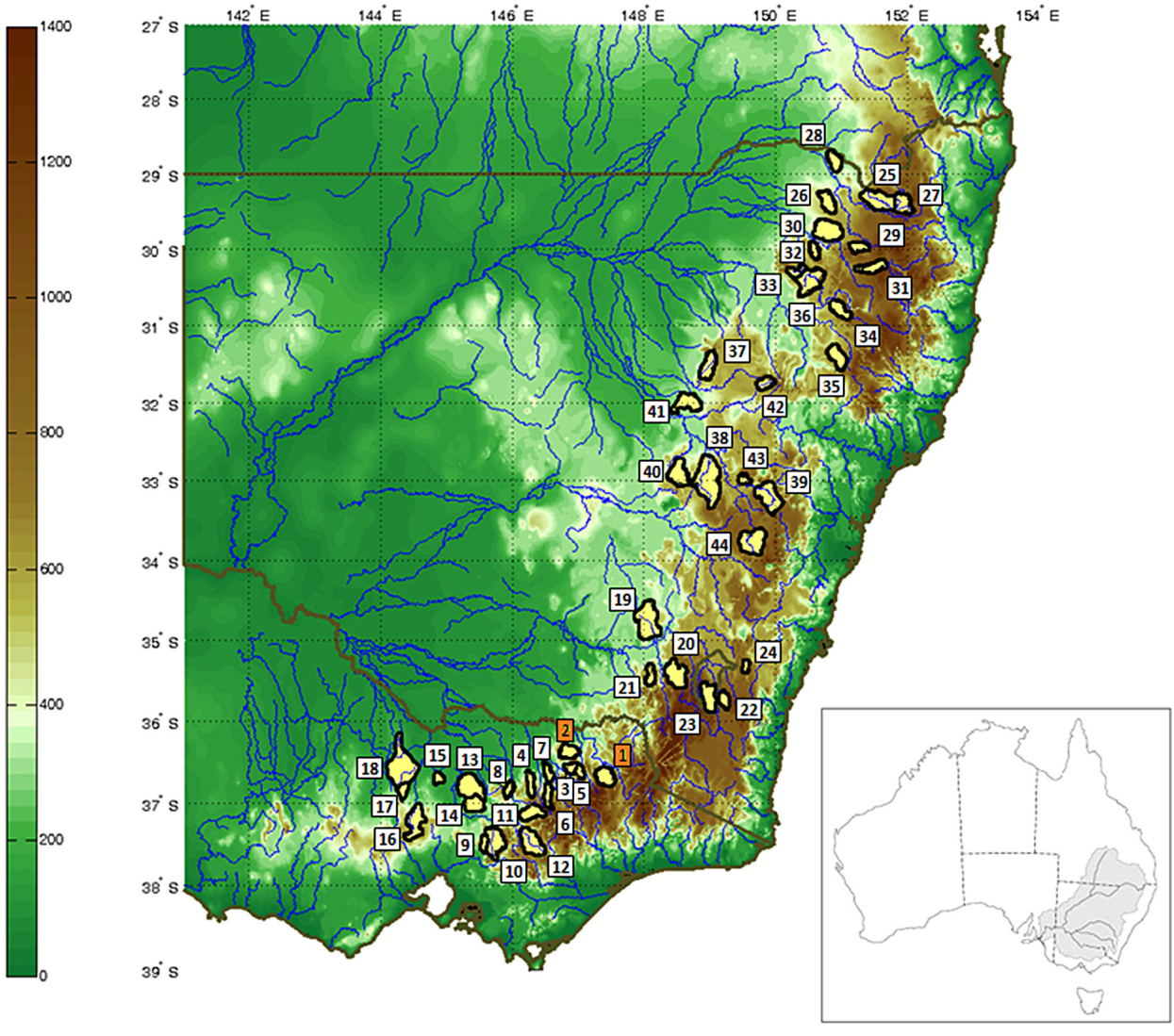

Figure 1. Location of the 45 catchments in the Murray Darling Basin considered in the study. The catchment numbers in the figure correspond to the IDs in Table 1. The two representative catchments catchment 401210 (1) and catchment 402204 (2) are highlighted. The inset shows the location and size of the Murray Darling Basin.

moisture, it does point to the often complex interaction between the flood-producing rainfall event upon which the design storm concept is based, and a longer period of rainfall and evaporation which influences the catchment moisture state prior to this event.

[7] An alternative, and conceptually simpler, approach to accounting for antecedent moisture is to use a continuous rainfall-runoff modeling framework [*Blazkova and Beven*, 2002; *Cameron et al.*, 1999; *Lamb*, 1999; e.g., *Lamb and Kay*, 2004]. Unlike event-based models for design flood estimation in which design rainfall is used as the primary input, continuous rainfall-runoff models use continuous rainfall sequences at daily or subdaily time scales as the input. Such rainfall sequences may be based on point-based or catchment-averaged continuous rainfall measurements (for lumped models) derived from one or more rainfall gauges over a sufficiently long time. Alternatively, they can be based on synthetically generated continuous rainfall sequences that capture the statistics of the historical rainfall [*Cameron et al.*, 1999; *Cowpertwait et al.*, 2002; *Heneker et al.*, 2001; *Mehrotra and Sharma*, 2007; *Sharma and Mehrotra*, 2010; *Westra et al.*, 2012], and simulate the type of low-frequency variability that appears to modulate the decadal variability noted in extreme floods [*Pui et al.*, 2011]. The output from this modeling system is a continuous sequence of modeled runoff, and a frequency analysis is then performed on this modeled sequence to derive the design runoff values [*Blazkova and Beven*, 2002].

[8] In this paper we examine the implications of antecedent moisture on flood quantiles by using a continuous rainfall-runoff modeling framework. A nonparametric resampling approach is used to infer the flood magnitude which would have occurred assuming the dependence was lost between the magnitude of the flood-producing rainfall event and the rainfall sequence leading up to that event. The aim is not only to highlight the importance of both short-memory (day-to-day

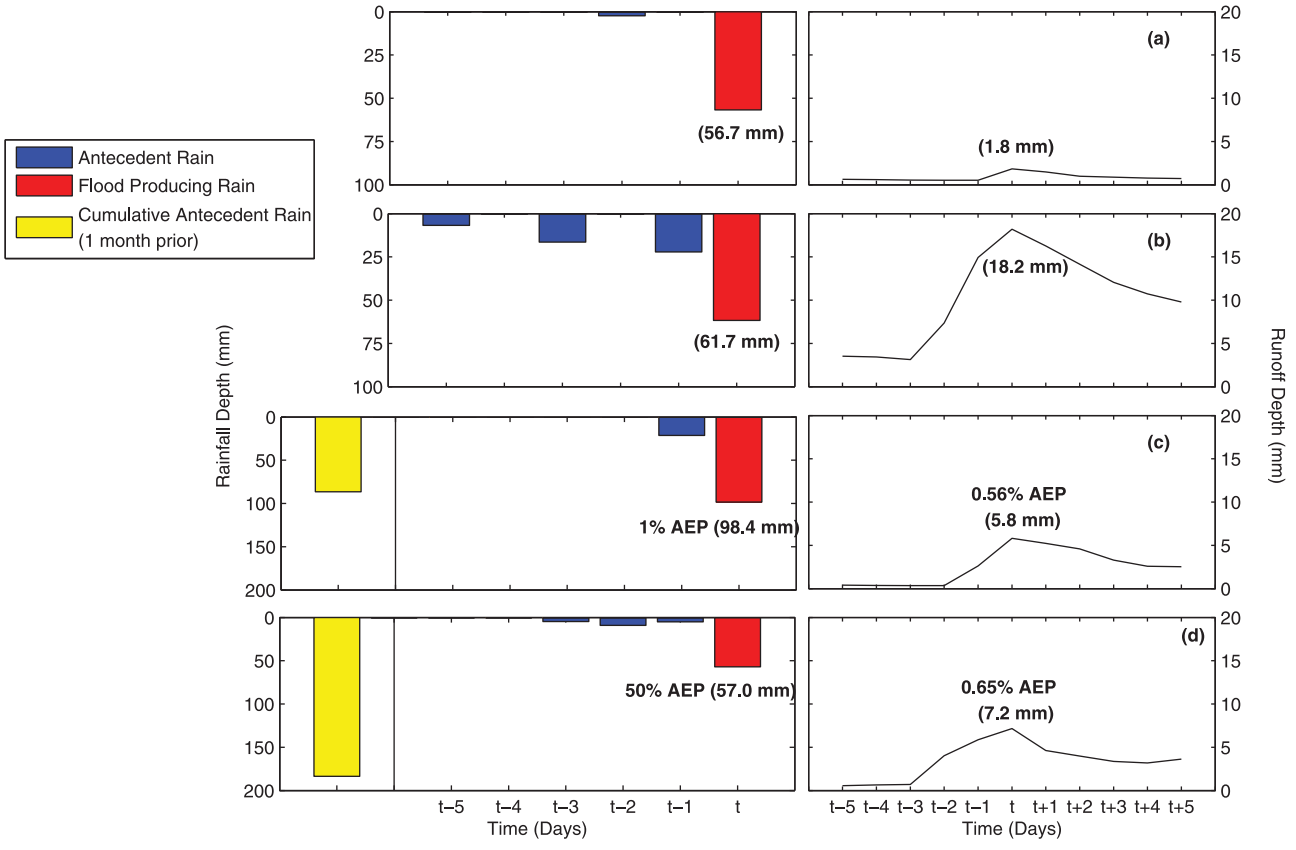

Figure 2. Selected observed flood events for a representative catchment (see catchment 401210 in Figure 1) indicating the importance of antecedent moisture. Although the magnitude of the flood producing rain is similar in (a) and (b), the resulting flood peak differs by almost a factor of 10, due largely to the difference in the week-long antecedent rainfall. However, (c) and (d) indicate that a doubling of the flood producing rain, with little variation in the cumulative week-long antecedent rainfall, can lead to a very similar magnitude of peak runoff. By and large, this is due to the combination of heavy (light) month-long antecedent rainfall with a smaller (larger) flood producing rain event. This indicates the need to consider a period of antecedent rainfall longer than the traditional 1–2 weeks in some cases.

dependence) and long-memory (seasonal or longer) rainfall processes in influencing the magnitude of the design flood event, but also to highlight the potentially significant biases which could arise if the joint probability between the design rainfall event and the antecedent wetness conditions were not properly taken into consideration. The antecedent rainfall is used as a surrogate measure of antecedent soil moisture as it is the primary factor (other than potential evapotranspiration) controlling soil moisture at depths which impact on rainfall to runoff conversion. This allows soil moisture to be accounted for using a relatively simple conceptual rainfall-runoff modeling framework, since explicit modeling of soil moisture will require accounting of soil and vegetation properties within a much more complex physical modeling approach. Given that the sources of large-scale climate variability which drive soil moisture variability at synoptic and seasonal time scales are the same as those which drive rainfall variability at those time scales [*Dirmeyer et al.*, 2009; *Douville*, 2003], the use of antecedent rainfall is likely to reasonably capture such persistence. Finally, in order to discern when a more demanding continuous methodology should be invoked, we aim to examine whether certain catchment attributes render the runoff response especially sensitive to the antecedent wetness state.

[9] The remainder of this paper is structured as follows. In section 2 we describe the data and catchments used for the study, along with an overview of the methodology used for resampling daily rainfall in order to evaluate the role of persistence in observed rainfall sequences. Section 3 summarizes the findings over all the test catchments, focusing particularly on the heavy events which are most important from a design perspective. The role of different objective functions in calibrating the rainfall-runoff model, as well as the role of different physiographic catchment characteristics in influencing the time period for which antecedent moisture is important, is also considered in this section. Finally, we conclude with a discussion of the implications of these results for the practice of design flood estimation.

2. Data and Methodology

2.1. Data

[10] The data for this study has been selected from a set of daily rainfall, potential evapotranspiration (PET) and gauged streamflow records from 240 catchments throughout the Murray Darling Basin (MDB). Catchment-averaged daily rainfall was used for each of the catchments, and was

based on the 5 km × 5 km gridded daily rainfall SILO database [*Jeffrey et al.*, 2001]. Monthly average PET data was based on the evapotranspiration maps published by the Australian Bureau of Meteorology as part of their Climate Atlas Series (see http://www.bom.gov.au/climate/how/newproducts/IDCetatlas.shtml), and both the rainfall and PET records have no missing values. The streamflow data set was obtained from work by *Vaze et al.* [2011], and comprises a quality-controlled set of gauged records in catchments that are largely unregulated and thus do not have any major storages or irrigation schemes. More than half the gauges have been recording since the early 1970s, with only 10% of catchments starting in the early 1980s or later. For the present study a subset of 45 catchments were ultimately selected as they have the most lengthy and complete records (all selected runoff records have less than 6% missing data), with record lengths ranging from 17 to 33 years. Figure 1 shows their locations in the MDB and Table 1 outlines other catchment details of interest. Despite a relatively low variability between catchments in the mean annual rainfall (coefficient of variation = 27%), the mean annual runoff varies considerably (coefficient of variation = 93%). The sensitivity of these catchments to small changes in annual rainfall is well known [*Chiew*, 2006], due to the high potential evaporation rates and comparatively low runoff coefficients particularly in the more northerly and inland parts of the domain. The catchment sizes range from 65 to 1629 km^2, and thus the response times for most of these catchments are shorter than one day. Nevertheless, daily averaged streamflow was used to ensure consistency with the rainfall data; this might result in an underestimation of the peak instantaneous flow rate, but is unlikely to have a significant bearing on the subject of this analysis which is the influence of antecedent rainfall in the days and months prior to the flood event on the flood hydrograph.

Table 1. Details of the 45 Catchments Considered for the Study

	Station	Location	Area (km^2)	Mean Annual Rainfall (mm)	Mean Annual Runoff (mm)	Record Length (yrs)
1	401210	Snowy Ck below Granite Flat, VIC	407	1212.4	463.9	33
2	402204	Yackandandah Ck at Osbornes Flat, VIC	255	1099.2	185.2	32
3	402206	Running Ck at Running Creek, VIC	126	1260.8	260.3	33
4	403213	Fifteen Mile Ck at Greta South, VIC	229	1138.7	254.0	33
5	403214	Happy Valley Ck at Rosewhite, VIC	135	1200.8	184.4	33
6	403217	Rose R at Matong North, VIC	154	1288.9	358.1	33
7	403224	Hurdle Ck at Bobinawarrah, VIC	155	983.0	178.9	33
8	404208	Moonee Ck at Lima, VIC	90.9	963.2	201.0	33
9	405205	Murrindindi R above "Colwells," VIC	108	1358.1	475.2	33
10	405209	Acheron R at Taggerty, VIC	619	1342.8	450.2	33
11	405214	Delatite R at Tonga Bridge, VIC	368	1143.4	291.4	33
12	405219	Goulburn R at Dohertys, VIC	694	1275.7	440.5	33
13	405226	Pranjip Ck at Moorilim, VIC	787	635.6	68.9	33
14	405228	Hughes Ck at Tarcombe Road, VIC	471	773.1	156.9	33
15	405229	Wanalta Ck at Wanalta, VIC	108	513.4	31.8	33
16	406213	Campaspe R at Redesdale, VIC	629	756.9	117.5	32
17	406214	Axe Ck at Longlea, VIC	234	583.5	56.3	32
18	407236	Mount Hope Ck at Mitiamo, VIC	1629	448.0	14.4	33
19	410044	Muttama Ck at Coolac, NSW	1025	659.3	42.1	32
20	410057	Goobarragandra R at Lacmalac, NSW	673	1172.5	413.6	32
21	410061	Adelong Ck at Batlow Road, NSW	155	1031.3	252.4	32
22	410141	Micaligo Ck at Michelago, NSW	190	738.4	38.1	23
23	410731	Gudgenby at Tennent, ACT	670	942.3	93.9	32
24	411003	Butmaroo Ck at Butmaroo, NSW	65	720.4	75.4	26
25	416008	Beardy River at Haystack, NSW	866	793.3	68.7	31
26	416020	Ottleys Ck at Coolatai, NSW	402	743.0	39.5	26
27	416023	Deepwater River at Bolivia, NSW	505	860.9	71.2	26
28	416036	Campbells Ck at Near Beebo, NSW	399	650.4	22.4	17
29	418005	Copes Ck at Kimberley, NSW	259	868.4	91.6	32
30	418017	Myall Ck at Molroy, NSW	842	737.5	33.3	27
31	418021	Laura Ck at Laura, NSW	311	803.2	79.9	27
32	418025	Halls Ck at Bingara, NSW	156	760.9	39.0	27
33	418027	Horton River at Horton Dam Site, NSW	220	904.3	176.5	31
34	419029	Halls Ck at Ukolan, NSW	389	759.0	42.3	27
35	419035	Goonoo Goonoo Ck at Timbumburi, NSW	503	802.6	50.1	24
36	419053	Manilla River at Black Springs, NSW	791	721.8	46.4	32
37	420010	Wallumburrawang Ck at Bearbung, NSW	452	696.2	21.3	22
38	421018	Bell River at Newrea, NSW	1620	717.9	60.9	32
39	421026	Turon River at Sofala, NSW	883	772.4	88.3	32
40	421048	Little River at Obley No.2, NSW	612	657.0	63.7	19
41	421055	Coolbaggie Ck at Rawsonville, NSW	626	587.6	34.6	25
42	421056	Coolaburragundy R at Coolah, NSW	216	690.3	58.0	18
43	421066	Green Valley Ck at Hill End, NSW	119	797.2	121.7	26
44	421101	Campbells River at Ben Chifely Dam, NSW	950	791.9	75.2	23
45	426504	Finniss River at 4 km east of Yundi, SA	191	834.0	128.0	32

2.2. Model Calibration

[11] In this study, the Australian water balance model (AWBM) [*Boughton*, 2004] is used as the rainfall-runoff model. The AWBM is a lumped conceptual water balance model that takes in rainfall and PET at daily or subdaily resolution, and uses three bucket storages. The model requires eight parameters to be specified, which are estimated during the calibration procedure.

[12] Fundamental to the study is the determination of flood response to variations in antecedent wetness. It is thus important to ensure that the parameters in the AWBM, particularly relating to catchment storage capacity are somewhat realistic. In order to achieve this, it is deemed necessary to calibrate on the full rainfall record, instead of just the peak flows which is common practice in design flood estimation.

[13] A calibration procedure is adopted which produces a single nominally global optimum parameter set. A goodness of fit measure is first chosen which places emphasis on simulating peaks since we are interested in the implications of antecedent moisture on the simulation of heavy flood events. The widely used Nash Sutcliffe coefficient of efficiency (NSE) is adopted as the objective function:

$$\mathrm{NSE} = 1 - \frac{\sum_{i=1}^{n} (\hat{\mathbf{Q}}_i - \mathbf{Q}_i)^2}{\sum_{i=1}^{n} (\mathbf{Q}_i - \overline{\mathbf{Q}}_i)^2} \tag{1}$$

where $\hat{\mathbf{Q}}$ is the vector of simulated flows, $\mathbf{Q}$ is the vector of observed flows, $\overline{\mathbf{Q}}$ is the mean of the observed flows, and n is the length of record. Although several limitations of this objective function have been highlighted in the literature (see for instance [*Jain and Sudheer*, 2008]), it is probably the most commonly used objective function in rainfall-runoff modeling for flood estimation applications due to the emphasis on high flows. Furthermore, a second objective function is considered so as to ensure that the results are not affected by calibration deficiencies (see section 3.3). The shuffled complex evolution algorithm (SCE-UA) [*Duan et al.*, 1993] is used as the search algorithm, with 10 different randomly generated parameter sets used to initialize the algorithm. Of the 10 resulting optimum parameter sets, the one corresponding to the highest NSE is chosen as representing the estimate of the global optimum.

[14] Figure 3 summarizes the calibration performance of all of the catchments, indicating that approximately 50% have an NSE greater than or equal to 0.7. The poor performance among some catchments could not be correlated to any basic catchment descriptor such as location or catchment size. It is likely that this is due to the often irregular response behavior associated with semiarid catchments, and the inability of the model to properly simulate this behavior. Although more complex dynamical modeling approaches are better equipped to consider the spatiotemporal resolution of the data [see for instance [*Salamon and Feyen*, 2009], and more detailed procedures exist to allow modeling of input [*Chowdhury and Sharma*, 2007; *Kavetski et al.*, 2006] and structural model uncertainty [*Marshall and Sharma*, 2006; *Renard et al.*, 2010], we do not consider these approaches since calibration is not the

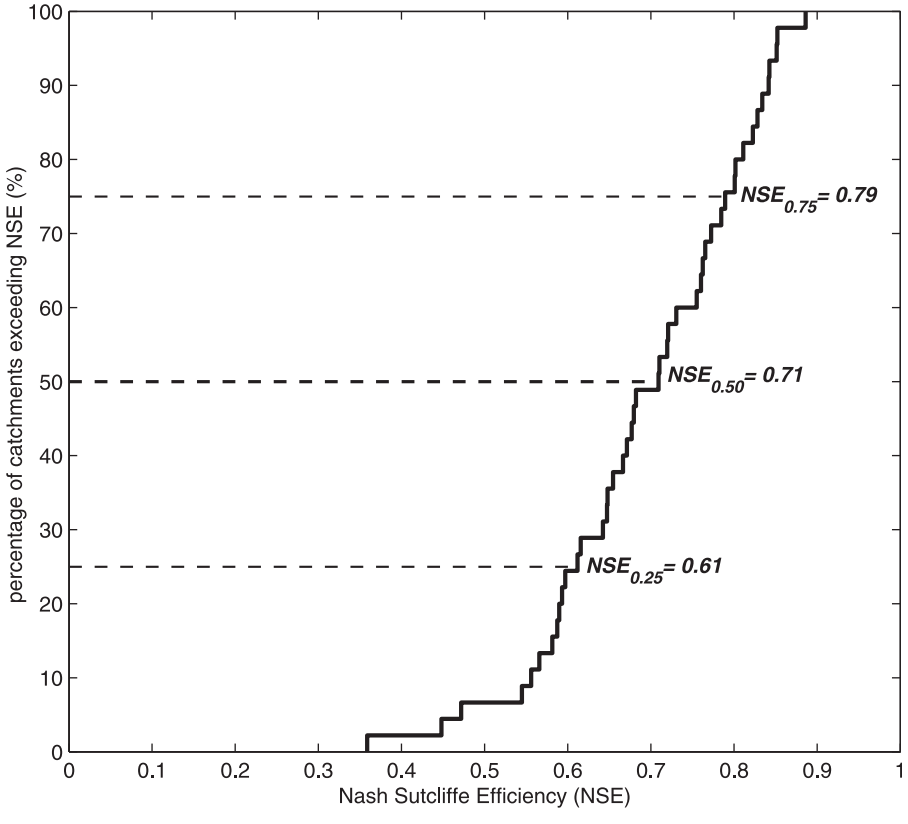

Figure 3. Distribution of calibration performance for all 45 catchments. A reasonable Nash Sutcliffe efficiency (NSE) is obtained across most catchments, with approximately half of the catchments having a NSE greater than or equal to 0.7.

focus of the study. This level of overall performance among the catchments is deemed acceptable, and any parameter uncertainties have been dealt with through the use of a large sample of catchments and multiple objective functions (for details see section 3.3). However, it is still necessary to determine whether the calibrated model will produce reasonable simulations when resampled rainfall is used. In order to determine model performance on noncalibration data, split sample validation is carried out on two representative catchments, catchment 401210 and catchment 402204. Table 2 shows that the NSE for calibration is within ± 0.1 of the NSE for the validation period for both catchments and for various calibration/validation splitting. We can thus be fairly confident that the model is suitably calibrated to take resampled rainfall inputs.

2.3. Estimating the Influence of Antecedent Conditions

[15] Having calibrated the AWBM for each catchment, we examine the importance of antecedent moisture in design flood estimation. To this end we use a method which is capable of determining the change in peak flow rate when antecedent moisture is not properly accounted for. We achieve this via a bootstrapping methodology to create rainfall sequences which maintain the same statistics of historical rainfall, except that the exact sequencing of rainfall leading up to the flood-producing rainfall event is rearranged to eliminate any serial dependence that might be present otherwise. This is done by ensuring that rainfall dependence at daily to interannual time scales is removed, by resampling the rainfall across all years for each day of the year. The specifics of the resampling algorithm are discussed in greater detail in the remainder of this section.

[16] The first step in the resampling process involves generating a full flow sequence from the historical rainfall data using the calibrated hydrologic model. Records for each variable (rainfall, PET and simulated runoff) are represented as 365 by n matrices ($\mathbf{R}$, $\mathbf{P}$, and $\widehat{\mathbf{Q}}$, respectively), where the hat notation is used to indicate that the streamflow sequence is derived from the calibrated model. Each row represents a calendar day indexed by i (ignoring leap days) and each column represents the year of record indexed by j, up to a total of n years of record. Here and in the remainder of this paper we use lower case italics for scalar quantities, upper case for vectors, and upper case bold for matrices. From the simulated flow sequences, a vector of annual maximum flows for each year j, represented as $\widehat{M}_j$, is estimated as

$$\widehat{M}_j = \max\{\widehat{\mathbf{Q}}_{1,j}, \ldots, \widehat{\mathbf{Q}}_{365,j}\}. \quad (2)$$

[17] We then proceed to resample the rainfall sequence prior to each day corresponding to the annual maximum runoff event. To do this we start by rewriting the sequence of rainfall prior to the annual maximum event as

$$W_j = \{r_{\max,j-z}, \ldots, r_{\max,j}\}, \quad (3)$$

where $r_{\max,j}$ represents the rain day coinciding with $\widehat{M}_j$ for each year, and z represents the number of years prior to $r_{\max,j}$ for which we want to consider the antecedent rainfall pattern. In this study we use $z = 3$ years (1095 days), which when used as an input to AWBM results in reproducing $\widehat{\mathbf{Q}}$ almost exactly. We use $z = 3$ years in order to be able to determine if low frequency variability at an interannual scale impacts on the design flood.

[18] For the remainder of this paper we use an equivalent way of expressing equation (3) as follows:

$$W_j = \{w_{1,j}, \ldots, w_{1095,j}\}, \quad (4)$$

where the series $w_{1,j}, \ldots, w_{1095,j}$ represents a continuous sequence of rainfall up to 1095 days (three years) prior to the annual maximum runoff event $\widehat{M}_j$.

[19] The next step is to generate a new rainfall matrix $\mathbf{R^{*b}}$, which is given by

$$R_j^{*b} = \{R_1^{*b}, \ldots, R^{*b}{}_{365}\}^T, \quad (5)$$

where R_j^{*b} is a vector forming the jth column of the matrix $\mathbf{R^{*b}}$, the superscript T indicates the transpose operator and the notation indicates that the resampling is performed separately for each day i. The resampling is carried out with replacement from the pool of n years. Implicit in any bootstrapping methodology is the need to create multiple realizations, and the same is done here by creating a total of $b = 1, \ldots, 100$ bootstrap replicates $\mathbf{R^{*b}}$. By doing this we obtain flood estimates by considering the full distribution of antecedent moisture values, instead of just one single antecedent moisture state. A new sequence W_j^{*b} is then developed from $\mathbf{R^{*b}}$, similar to equation (4) but drawing from $\mathbf{R^{*b}}$ instead of $\mathbf{R}$.

[20] The algorithm can thus be summarized as follows:

[21] (i) For each simulated annual maximum runoff event ($\widehat{M}_j$), construct a sequence of rain days leading up to this event, given by equation (4). Similarly, construct the 100 bootstrapped replicates W_j^{*b}.

[22] (ii) Input the following rainfall sequence: $\{w_{1,j,\ldots,}^{*b}$ $w_{1095-k-1,j,}^{*b} w_{1095-k,j,\ldots,} w_{1095,j}\}$ to the rainfall-runoff model, where the notation indicates that the first $1095-k$ days have been generated using the bootstrap with replacement procedure, with the last k days prior to the annual maximum runoff event being fixed. This is repeated for $k = 0, \ldots, 1095$ days such that an increasing number of days are being held fixed prior to the observed runoff event.

Table 2. Split Sample Calibration (C)/Validation (V) Results for Catchment 401210 and Catchment 402204

Catchment 401210			Catchment 402204		
Calibration/Validation %	NSE(C)	NSE(V)	Calibration/Validation %	NSE(C)	NSE(V)
30/70	0.874	0.797	30/70	0.680	0.634
50/50	0.832	0.729	50/50	0.663	0.704
70/30	0.833	0.778	70/30	0.669	0.673

[23] (iii) Input each sequence to the model individually, after which the last day of simulated runoff is extracted and given as M_j^{k*b}.

[24] Having carried out these steps, we end up with a total of 100 replicates of the annual maximum runoff series M^* for any particular k, where M^* is a vector of values of M_j^{k*b}, for $j = 1$ to n. A flood frequency analysis is then performed on the annual maximum runoff series to obtain design flood estimates resulting from the use of resampled rainfall. Since the distribution of M^* is unknown, we work with the empirical cumulative distribution function to avoid having to assume a particular form of a distribution. The flood frequency analysis is also carried out on the "true" simulated annual maxima series M.

[25] We then summarize the multitude of data by taking the median of the x% AEP runoff over all trials for all $k = 1, 2, \ldots, 1095$. A relative error statistic given below is then used to quantify the change in flood estimates for various exceedance probabilities:

$$\text{relative error}\,(\%) = \left(\frac{Q_r - Q_a}{Q_a}\right) \times 100, \tag{6}$$

where Q_r = median runoff (over all trials) for the x% AEP and given k and Q_a = runoff for the x% AEP when the continuous historical rainfall sequence is used. It can be seen from the equation that negative values of the relative error indicate an underestimation of the runoff, while positive values indicate an overestimation.

3. Results and Discussion

3.1. Role of Antecedent Precipitation

[26] Initially we consider the flood frequency relationships that result from various lengths of the rainfall sequence held fixed prior to the annual maximum flow day; in other words, different values of k. This is documented for a single representative catchment (catchment 402204, see Figure 1) in Figure 4, which clearly indicates that the design flood values are underestimated when the period of antecedent rainfall considered is too short (that is, the value of k is too small). As expected, the amount of underestimation reduces as k increases. This does not occur equally for all catchments due to a high degree of variability across trials and a high sensitivity to day-to-day variations in the input rainfall sequence. The amount and direction of change to the flood frequency curves from the different input rainfall sequences (as described by the relative error statistic detailed in section 2.3) also varies across catchments. As a result, we turn to summarizing the change in the flood frequency curves by considering the mean over all catchments examined in the MDB for the 2%, 5%, 10%, and 20% AEP event.

[27] Figure 5 shows the result for $k = 0, 1, 2, \ldots, 250$, where convergence to zero is attained at roughly $k = 250$ days. The data has been smoothed to remove random noise using a Savitzky-Golay moving average (a least squares polynomial smoothing, for details see *Savitzky and Golay* [1964]), with a polynomial of degree 2. We used this more sophisticated moving average instead of a simple moving average because of its ability to preserve higher order moment characteristics in the data, including the position of peaks. In order to preserve the sharper reduction in relative error for very small k values, the smoothing has not been carried out on data points corresponding to $k = 0$ to 4.

[28] Figure 5 clearly shows that on average there is a consistent underestimation of the design flood across all exceedance probabilities when antecedent moisture is not properly accounted for. This can be attributed to the dependence structure in rainfall, in which wet days tend to follow wet days and dry days tend to follow dry days. The resampling removes this dependency, so that the antecedent catchment moisture is reduced thus leading to less runoff from the flood-producing rain event. The exceedance probability contours also indicate that accounting for antecedent moisture becomes less important as the exceedance probability of the event decreases. This conforms to our expectation that in general, for higher runoff events, the impact of antecedent moisture on the resulting runoff is diminished because of the size of the event relative to the catchment storage. This is contrary to smaller runoff (and thus more frequent) events, where the magnitude of the runoff may be comparable to the size of the storages, and thus can be more significantly affected by antecedent moisture conditions.

[29] We also note that the exceedance probability contours in Figure 5 all have a relatively steep gradient between $k = 0$ and $k = 4$ (particularly between $k = 0$ and $k = 1$). This behavior is attributed to the low order Markovian dependence (order 1 and 2) in rainfall, which is commonly assumed to be the dominant and thus most important means of capturing persistence [*Sharma and Mehrotra*, 2010]. This is reinforced here with improvements in accuracy of around 20% attained when two days of antecedent rainfall are considered compared to none. However, these results indicate that higher order dependencies in rainfall must also be considered, with underestimation of flood magnitudes still occurring at seasonal time scales. In fact, more than 50% of catchments require in excess of three months of prior rainfall to be considered in order to reduce the relative error to less than 5%, as shown in Table 3. In contrast, the impact of lower frequency (interannual and longer time scale) variability in rainfall on antecedent moisture is not all that apparent since flood estimates with a negligible reduction in accuracy can be achieved by considering less than a year of antecedent rainfall.

3.2. Relationship With Catchment Attributes

[30] We now consider whether certain catchment characteristics render the runoff response especially sensitive to antecedent moisture. The formation of such relationships will be advantageous in that a more complex continuous simulation methodology can be adopted only when necessary, based on the catchment's characteristics. Hence we consider the implications of a range of physiographic and antecedent precipitation characteristics on the sensitivity to antecedent moisture, as detailed in Table 4. Here our catchment characteristics are a combination of measurable quantities (e.g., size) as well as model parameters (e.g., base flow index). Although such model parameters do not correspond to any single physically measurable attribute, they provide a way for quantifying the impact of a combination of physiographic characteristics on a complex process, such as the soil type, vegetation cover, and so on that will impact on the conversion of excess rainfall to runoff.

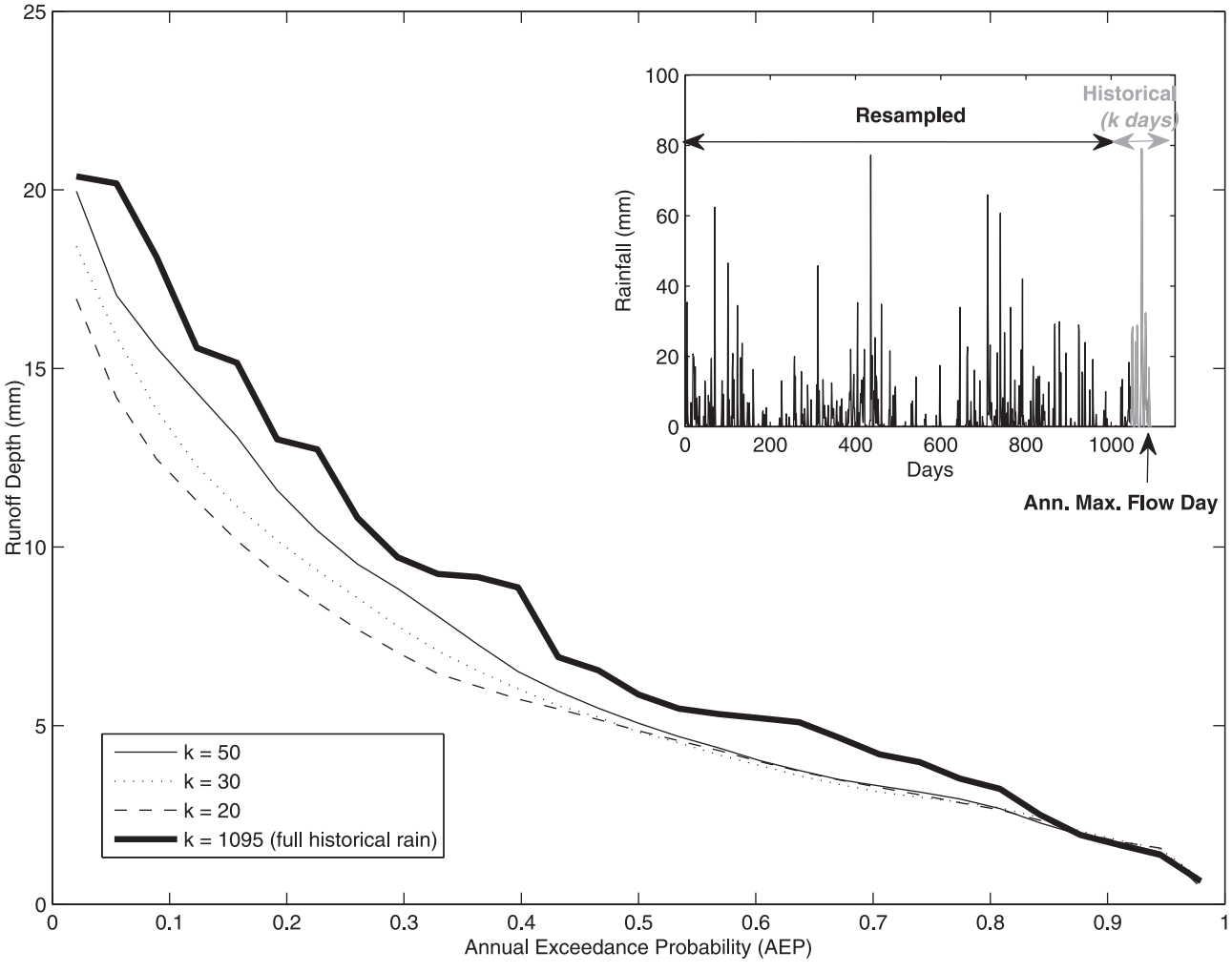

Figure 4. Flood frequency relationships from bootstrapped sequences of various k values for a representative catchment (see catchment 402204 in Figure 1). Note how the flood frequency curves approach the thick line (i.e., when the full rainfall sequence is used) as k increases. The figure in the inset represents an example of a single bootstrapped rainfall sequence for $k = 50$. Here the 50 days prior to the day of the annual maximum flow are equivalent to the historical record, while the remaining portion is a resampled sequence.

[31] We begin by regressing the impact of catchment size on various measures of the magnitude of runoff underestimation. This is done because we expect the longer time of concentration associated with larger catchments to lead to the runoff response being more sensitive to longer time scales of antecedent rainfall. A linear regression framework is used throughout this analysis as visual inspection of the relationships did not indicate any strong supporting evidence of nonlinear behavior, with model residuals being approximately normally distributed and homoskedastic.

[32] Surprisingly, we do not find any statistically significant relationships between catchment size and the underestimation of runoff, possibly due to the majority of catchments having times of concentration well under a day. As a result, we consider a larger range of predictor variables given in Table 4 in a multiple linear regression which allows us to determine which predictors impact most significantly on a catchment's sensitivity to antecedent moisture at various time scales. The statistical significance of the resulting linear relationships is determined through a standard t-distribution-based hypothesis test. These results are summarized in Figure 6, along with the sign of the correlation for each of the predictors.

[33] First, we note that it is mainly the antecedent rainfall predictors (MR_30, MR_60, and MR_120) which impact on the relative error (described by the R0 and R1 statistics). They are in general positively correlated, indicating that increases in the expected value of antecedent rainfall lead to a decrease in the degree to which the flood peaks are underestimated. In other words, the necessity to consider antecedent rainfall in the flood estimation process reduces as the amount of rainfall prior to the flood producing event increases. This phenomenon is due mostly to the correlation between antecedent rainfall and the flood producing event (see Figure 7), meaning that greater antecedent rainfall is linked with larger flood producing storms which tend to dominate the runoff response and dampen the impact of antecedent moisture conditions. *Cordery* [1970] also established

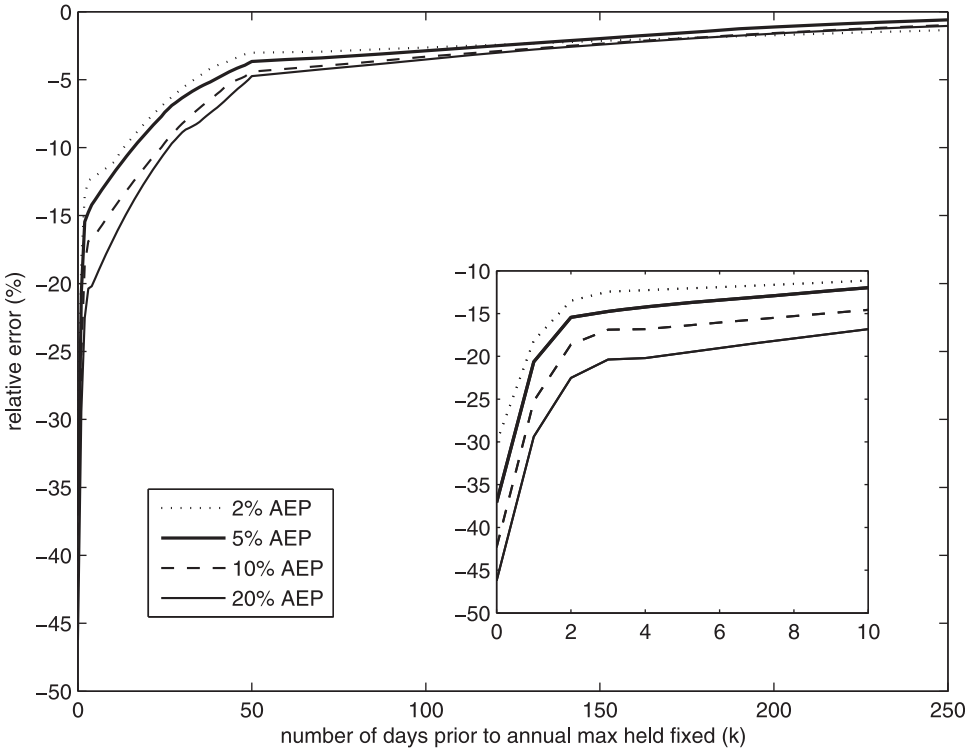

Figure 5. Relative error (%) versus number of days prior to the annual maximum flow day held fixed (k), taking the mean over all catchments (with inset showing the first 10 days only). There is a clear underestimation of all flood events when antecedent moisture is not considered. It can also be seen that the extent of underestimation reduces as the frequency of the event reduces.

a link between rainfall and sensitivity to antecedent moisture, stating that the assumption that antecedent wetness is unimportant "is reasonable for areas where the mean annual rainfall exceeds 50 inches [1270 mm]."

[34] We also notice that across the range of exceedance probabilities, the routing parameters (KBF and KSURF) consistently control the length of antecedent rainfall that is required for an accurate flood estimate (described by the K5 and K10 statistics). The results indicate that as the routing parameters increase toward 1 (which indicates increased lagging of the base flow or surface runoff), the number of days of antecedent rainfall (k) that needs to be considered increases. If a catchment's runoff response is characterized by significant lagging, then it is likely that the larger flood events will have had a sizable contribution from earlier rainfall events. This then justifies the need to include a longer period of antecedent rainfall to better characterize the state of the catchment storages, including the base flow stores which contribute slower moving groundwater to streamflow. Since these routing parameters embed a range of physical catchment characteristics (such as area, drainage density, soil type, catchment roughness, slope), it is difficult to isolate the impacts of such physically real catchment attributes on the sensitivity to antecedent moisture. Instead, we can conclude that if it is expected that the arrival of the flood peak experiences significant lag, then it would be wise to consider a continuous simulation methodology which is capable of accounting for a lengthy period of antecedent rainfall.

Table 3. Percentage of Catchments Which Fall Into Various Ranges of k (Days) Needed for the Relative Error to Reduce to Less Than 5% for Various Exceedance Probabilities[a]

		Annual Exceedance Probability			
	k (days) at RE < 5%	2%	5%	10%	20%
Short memory	0–7	18.8%	21.9%	15.6%	0
Long memory	8–90	56.3%	53.1%	65.6%	75%
	91–180	6.3%	12.5%	9.4%	9.4%
	181+	18.8%	12.5%	9.4%	15.6%

[a]Across all exceedance probabilities more than 50% of catchments require several months (up to 3 months) of prior rainfall to be considered to properly simulate the antecedent profile, demonstrating the importance of considering long-memory processes in rainfall.

[35] Unfortunately, the results of Figure 6 indicate that we can only make qualitative conclusions regarding when continuous simulation should be invoked. This is because the variation in predictors across exceedance probabilities and response statistics makes it difficult to arrive at a general set of important catchment attributes and how these interact to govern the rainfall-runoff relationship. In particular, there is a difficulty in representing the interconnected rainfall-to-runoff conversion mechanisms, many of which are not fully understood, through simple relationships involving catchment characteristics. Several studies into regionalization techniques, which inherently assume a link between hydrologic and physical similarity, have identified this issue [see for instance [*Oudin et al.*, 2010; *Reichl et al.*, 2009] thus explaining the lack of clear relationships

Table 4. Predictor and Response Variables Used in the Multiple Linear Regression

	Predictor Variables		Response Variables	
	Name	Definition	Name	Definition
Antecedent Rainfall Statistics	MAR	Mean Annual Maximum Rainfall	R0	Relative Error (%) for $k = 0$
	MR_30	Mean 30 days prior Rainfall[a]	R1	Relative Error (%) for $k = 1$
	MR_60	Mean 60 days prior Rainfall [a]	R30	Relative Error (%) for k= 30
	MR_120	Mean 120 days prior Rainfall [a]	K10	k (days) when Relative Error = 10%
Catchment Attributes	AREA	Catchment Area	K5	k (days) when Relative Error = 5%
	CAS	Catchment Average Storage[b] $= \sum_{i=1}^{3} C_i A_i$ where C_i = storage capacity, A_i = partial area fraction		
	BFI	Baseflow Index[b]		
	KBF	Baseflow Recession Coefficient[b]		
	KSURF	Surface Runoff Recession Coefficient[b]		

[a]Mean of the values prior to the annual maximum flow day.
[b]Parameter in AWBM.

from the regression analysis. As a result, based on catchment characteristics alone, it is difficult to determine a priori which catchments are more likely to be heavily influenced by antecedent moisture, and thus this will need careful examination on a case-by-case basis.

3.3. Implications of Assumptions

[36] It is important to note that the results presented earlier are based on simulated runoff as opposed to observed flow values. We selected this approach to ensure internal consistency in evaluating the difference between the original rainfall sequences and the resampled sequences. To evaluate the implications for different sets of "optimal" model parameters on the results presented in Figure 5, we now calibrate the model using an alternative objective function. This is done by repeating the analysis described in section 2, but this time using a peak over threshold calibration. This method involves calibrating only on flows above a threshold (determined so that there are on average roughly five flood peaks per year), thus placing greater

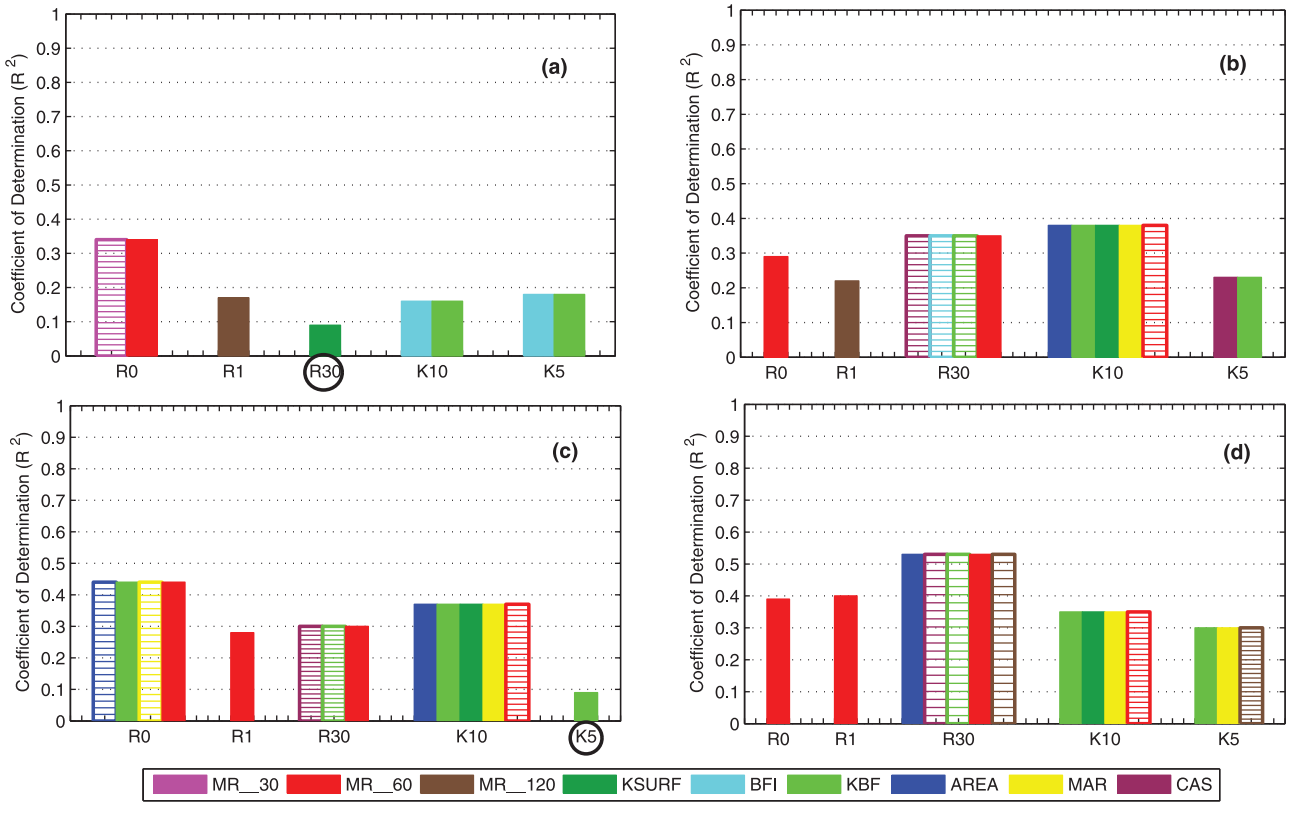

Figure 6. Optimum sets of predictors for various response variables for (a) 2% AEP, (b) 5% AEP, (c) 10% AEP, and (d) 20% AEP. The black circles indicate response variables for which no statistically significant relationship was found. The hatched pattern indicates a negative correlation with that predictor, while the solid fill indicates a positive correlation.

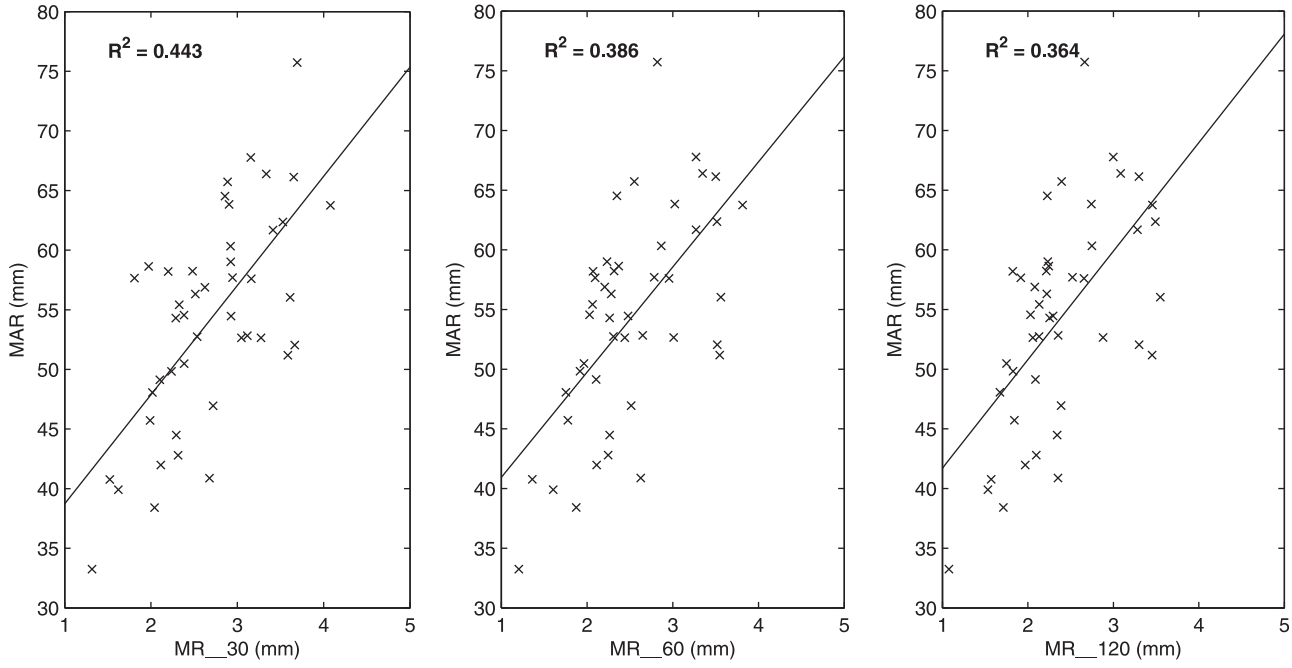

Figure 7. Correlation between mean of the annual maximum rainfall event and antecedent rainfall statistics (mean 30, 60, and 120 days prior to the annual maximum event). All three plots indicate that increases in the antecedent rainfall statistics lead to, on average, increases in the expected annual maximum event.

emphasis on ensuring the peaks are simulated correctly as shown in Figure 8. The remainder of the analysis follows the same procedure as described earlier, and the results are presented in Figure 9.

[37] As can be seen, Figure 9 is very similar in appearance to the relative error for various k values when the original parameter sets are used. First, it shows the same consistent underestimation of runoff across all exceedance probabilities, when antecedent moisture conditions are not properly accounted for. The magnitude of underestimation for corresponding exceedance probabilities is also quite similar, along with the time scales of antecedent rainfall which are needed for accurate flood estimates (negligible relative error is achieved for the same $k = 250$ in the original case). It also shows a similar trend of increasing absolute value of the relative error as the exceedance probability increases, which was evident in Figure 5. The remarkable similarity of the results obtained when a different objective function is used for calibration adds confidence to our conclusions.

[38] In section 3.1 we noted that the underestimation of the design flood demonstrated in Figure 5 was a result of the resampling method removing the dependence structure in the rainfall. In order to fully justify this statement, we consider a second resampling technique which considers the day to day dependence in the rainfall, but still does not capture less frequent modes of variability. Specifically, a nonparametric k-nearest neighbor conditional bootstrap scheme assuming Markov order 1 dependence is used (for full details, see *Lall and Sharma* [1996]). In this method, resampling for day t is conditional on day $t + 1$, with a moving window of ± 15 days across all years (as recommended by *Mehrotra and Sharma* [2007]). We aim to reproduce Figure 5, using the same methodology described earlier except with rainfall sequences from this nearest neighbor resampler.

[39] Figure 10 shows the results from this exercise, along with the results from Figure 5 superimposed for the purposes of comparison. It is clear that for all k, the magnitude of the relative error is smaller when the conditional resampler is used. This is in accordance with the statement that the underestimation seen in Figure 5 was due in large part to the dependence structure in the rainfall sequence being removed. Furthermore, both resamplers require roughly the same k until convergence of the relative error to zero (approximately $k = 250$). This again confirms the importance of long memory in rainfall (discussed in section 3.1) since although the conditional bootstrap maintains day-to-day dependence, it still removes the interannual variability (as does the original bootstrap method). Lastly, the conclusion that antecedent wetness plays a more important role in more frequent events is affirmed, as Figure 10 also shows the magnitude of relative error reduces as the AEP reduces when the k-nearest neighbor resampler is used.

[40] We also note that several simplifications have been employed in order to arrive at these conclusions, although it is not expected that they would impact dramatically on our results. For instance, the results presented above have been obtained using only a single rainfall-runoff model, namely the AWBM. We would expect that using multiple model structures and more complex semidistributed or distributed models (which consider spatial variations in the input variables), might result in quantitative differences in the degree to which flood runoff is underestimated by not properly accounting for antecedent moisture. Nevertheless, an underestimation of the heavy events when antecedent

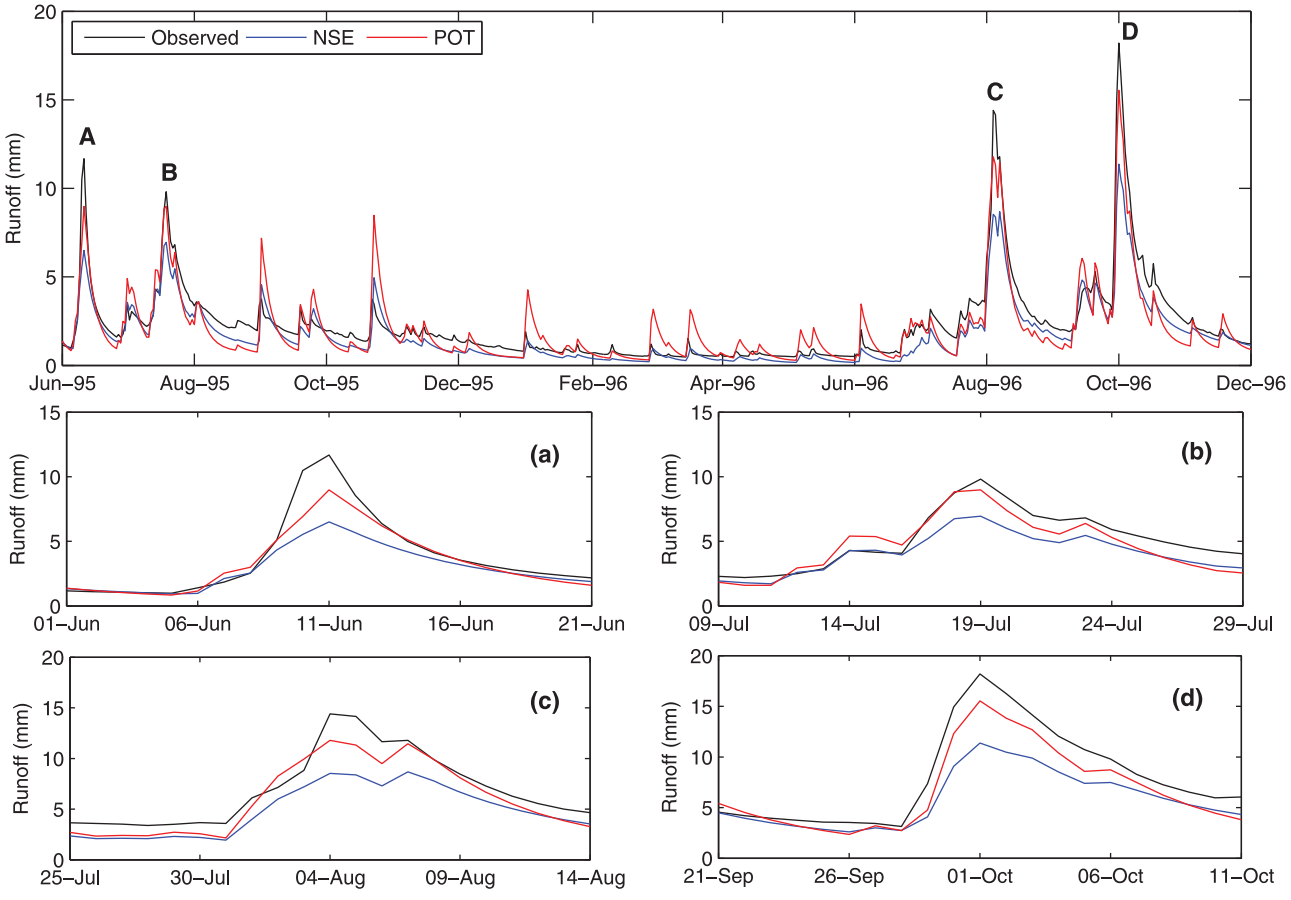

Figure 8. Calibration performance for the peak over threshold calibration (POT) and the original full series calibration (NS) for catchment 401210 (as shown in Figure 1). (a) to (d) are examples of heavy events for which the peak over threshold calibration clearly outperforms the full series calibration.

moisture is not properly simulated, along with the importance of considering short- and long-memory dependencies in rainfall, would still be expected across most models. Overall, the necessity for a continuous simulation methodology to correctly model antecedent moisture would still be apparent.

4. Conclusions

[41] By considering a resampling methodology which removes the dependence structure in rainfall, we examined the importance of antecedent moisture in determining the magnitude of the design flood. The study showed that the magnitude of heavy events (2%, 5%, 10%, and 20% AEP) in the test catchments is on average underestimated when the joint dependence between the flood-producing rain event and antecedent wetness state is not considered. Given the increasing concern about nonstationarity in rainfall sequences [*Milly et al.*, 2008; *Westra and Sisson*, 2011; *Westra et al.*, 2010] and likely changes to both average annual rainfall and rainfall extremes [*Bates et al.*, 2008], the study also highlights the need to carefully consider future changes in the joint probability between antecedent wetness and the flood-producing rain event, which would be difficult to capture in traditional event-based modeling approaches. This draws attention to an important limitation in traditional design flood estimation methods and the need to move toward approaches which more accurately model antecedent moisture.

[42] The study also demonstrated the importance of both short-memory (day-to-day) and long-memory (monthly and seasonal) time scales in rainfall and its impacts on antecedent moisture and the resulting flood peak. We noted that, as expected, short-memory had the greatest impact on the resulting flood, due to the accuracy of flood estimates improving by roughly 20% when 2 days of prior rainfall are considered compared to none. However, there was on average a 5% underestimation of flood flows even when simulating several months of antecedent rainfall, highlighting that catchment moisture conditions can exert a long-term control on flood frequency. This also reinforces the importance of ensuring stochastic rainfall generation techniques capture not only day-to-day dependence (as is done by low order Markov models), but also seasonal and longer term persistence [e.g., *Mehrotra and Sharma*, 2007]. Further support to this hypothesis is provided by *Pui et al.* [2011] who found that low-frequency variability in the rainfall preceding annual maximal events is a direct cause of similar low-frequency variability in the ensuing flood values. A continuous simulation approach which considers persistence structures in rainfall at such time scales is thus likely to offer some important benefits for design flood estimation through its ability to derive exceedance probability neutral estimates of design flood values.

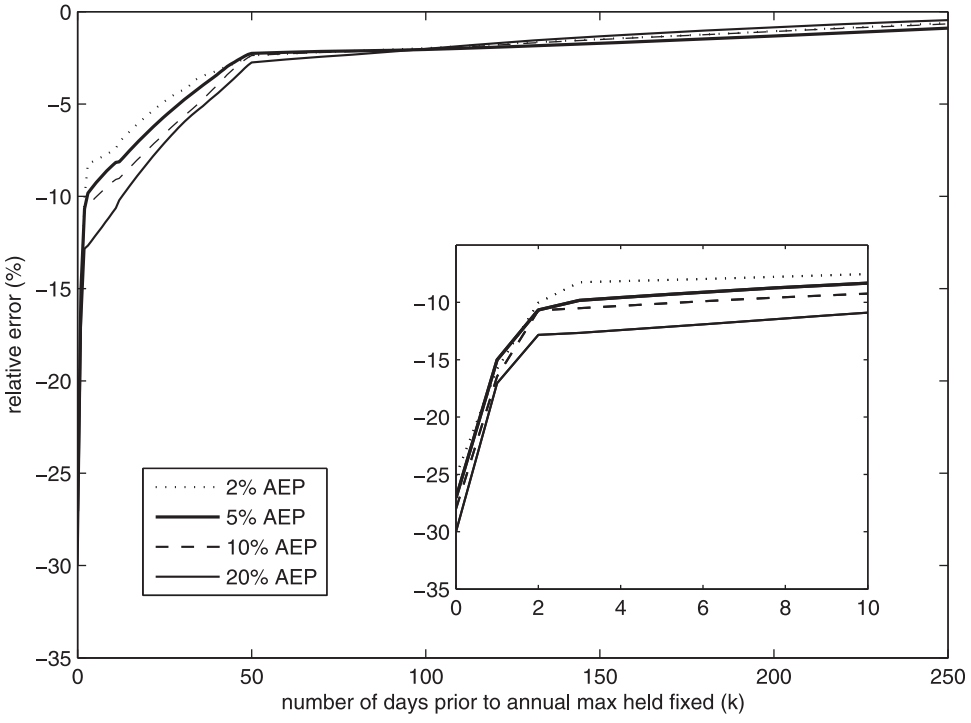

Figure 9. Relative error (%) versus k, taking the mean over all catchments, using the peak over threshold calibration. The same trends identified in Figure 5 are also apparent here.

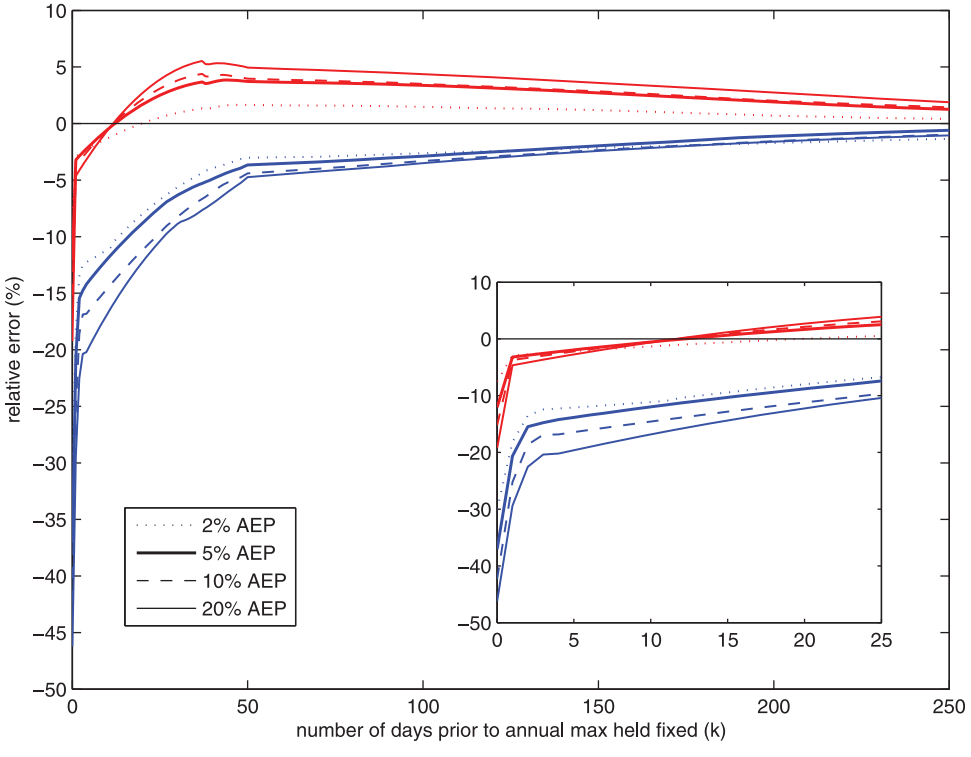

Figure 10. Relative error (%) versus k, taking the mean over all catchments using the two resampling techniques. The red lines indicate the results from the k-nearest neighbor conditional bootstrap, while the blue lines indicate the results from the original bootstrapping technique described in section 2.3. The magnitude of the relative error is clearly reduced for all k when the day to day dependence is accounted for (i.e., the conditional bootstrap is used).

[43] **Acknowledgments.** Partial funding for this research was generously provided by the National Climate Change Adaptation and Research Facility (NCCARF), the Australian Research Council, and the Australian Rainfall and Runoff revision project funded by the Department of Climate Change to the Institution of Engineers, Australia. Their support for this work is greatly acknowledged. Data for this study was generously provided by Jai Vaze.

References

Bates, B. C., Z. W. Kundzewicz, S. Wu, and J. P. Palutikof (2008), *Clim. Change* and Water, Technical Paper of the Intergovernmental Panel on *Clim. Change Rep.*, 210 pp., IPCC Secretariat, Geneva.

Beven, K. J. (2002), *Rainfall-Runoff Modelling: The Primer*, 360 pp., John Wiley, New York.

Blazkova, S., and K. Beven (2002), Flood frequency estimation by continuous simulation for a catchment treated as ungauged (with uncertainty), *Water Resour. Res.*, *38*(8), 1139, doi:10.1029/2001WR000500.

Bloschl, G. (2005), Rainfall-runoff modeling of ungauged catchments, in *Encyclopedia of Hydrology Science*, edited by M. G. Anderson. (Available at http://onlinelibrary.wiley.com/doi/10.1002/0470848944.hsa140/abstract.)

Boughton, W. (2004), The Australian water balance model, *Environ. Model. Software*, *19*(10), 943–956.

Boughton, W., and O. Droop (2003), Continuous simulation for design flood estimation—A review, *Environ. Model. Software*, *18*(4), 309–318.

Cameron, D., K. Beven, J. Tawn, S. Blazkova, and P. Naden (1999), Flood frequency estimation by continuous simulation for a gauged upland catchment (with uncertainty), *J. Hydrol.*, *219*(3–4), 169–187.

Cameron, D., K. Beven, and P. Naden (2000), Flood frequency estimation by continuous simulation under climate change (with uncertainty), *Hydrol. Earth Syst. Sci.*, *4*(3), 393–405.

Chiew, F. H. S. (2006), An overview of methods for estimating climate change impact on runoff, in *30th Hydrology and Water Resources Symposium*, Launceston, Tasmania, December 2006, Engineers Australia, Barton, Aust. Capital Terr, (CD-ROM, ISBN 0-8582579-0-4).

Chowdhury, S., and A. Sharma (2007), Mitigating parameter bias in hydrological modelling due to uncertainty in covariates, *J. Hydrol.*, *340*, 197–204.

Cordery, I. (1970), Antecedent wetness for design flood estimation, *Civil Eng. Trans. Inst. Eng. Aust.*, *CE12*(2), 181–184.

Cowpertwait, P. S. P., C. G. Kilsby, and P. E. O'Connell (2002), A space-time Neyman-Scott model of rainfall: Empirical analysis of extremes, *Water Resour. Res.*, *38*(8), 1131, doi:10.1029/2001WR000709.

Dirmeyer, P. A., C. A. M. Scholsser, and K. L. Brubaker (2009), Precipitation, recycling and land memory: An integrated analysis, *J. Hydrometeorol.*, *10*(1), 278–288.

Douville, H. (2003), Assessing the influence of soil moisture on seasonal climate variability with AGCMs, *J. Hydrometeorol.*, *4*, 1044–1066.

Douville, H., S. Conil, S. Tyteca, and A. Voidoire (2007), Soil moisture memory and West African monsoon predictability: Artefact or reality?, *Clim. Dyn.*, *28*, 723–742.

Duan, Q. Y., V. K. Gupta, and S. Sorooshian (1993), Shuffled complex evolution approach for effective and efficient global optimisation, *J. Opt. Theory Appl.*, *73*(3), 501–521.

Heggen, R. (2001), Normalized antecedent precipitation index, *J. Hydrol. Eng.*, *6*(5), 377–381.

Heneker, T. M., M. Lambert, and G. Kuczera (2001), A point rainfall model for risk-based design, *J. Hydrol.*, *251*, 65–87.

Jain, S. K., and K. P. Sudheer (2008), Fitting of hydrologic models: A close look at the Nash-Sutcliffe Index, *J. Hydrol. Eng.*, *13*(10), 981–987.

Jeffrey, S. J., J. O. Carter, K. B. Moodie, and A. R. Beswick (2001), Using spatial interpolation to construct a comprehensive archive of Australian climate data, *Environ. Model. Software*, *16*(4), 309–330.

Kavetski, D., G. Kuczera, and S. W. Franks (2006), Bayesian analysis of input uncertainty in hydrological modeling: 2. Application, *Water Resour. Res.*, *42*(3), W03408, doi:10.1029/2005WR004376.

Koster, R., and M. Suarez (2001), Soil moisture memory in climate models, *J. Hydrometeorol.*, *2*, 558–570.

Kuczera, G., M. Lambert, T. M. Heneker, S. Jennings, A. J. Frost, and P. J. Coombes (2006), Joint probability and design storms at the crossroads, *Aust. J. Water Resour.*, *10*(1) 63–79.

Kuichling, G. (1889), The relation between the rainfall and the discharge of sewers in populous districts, *ASCE Trans.*, *120*, 1–56.

Lall, U., and A. Sharma (1996), A nearest neighbor bootstrap for resampling hydrologic time series, *Water Resour. Res.*, *32*(3), 679–693, doi:10.1029/95WR02966.

Lamb, R. (1999), Calibration of a conceptual rainfall runoff model for flood frequency estimation by continuous simulation, *Water Resour. Res.*, *35*(10), 3103–3114.

Lamb, R., and A. L. Kay (2004), Confidence intervals for a spatially generalized, continuous simulation flood frequency model for Great Britain, *Water Resour. Res.*, *40*(7), W07501, doi:10.1029/2003WR002428.

Marshall, L., and A. Sharma (2006), Modelling the catchment via mixtures: Issues of model specification and validation, *Water Resour. Res.*, *42*, W11409, doi:10.1029/2005WR004613.

Mehrotra, R., and A. Sharma (2007), Preserving low-frequency variability in generated daily rainfall sequences, *J. Hydrol.*, *345*, 102–120.

Milly, P. C. D., J. Betancourt, M. Falkenmark, R. M. Hirsch, W. Zbigniew, Z. W. Kundzewicz, D. P. Lettenmaier, and R. J. Stouffer (2008), Stationarity is dead: Whither water management? *Science*, *319*, 573–574.

Mulvaney, T. J. (1851), On the use of self-registering rain and flood gauges in making observation of the relation of rainfall and floods discharge in a given catchment, *Proc. Inst. Civil Eng. Ireland*, *4*, 18–31.

Oudin, L., A. Kay, V. Andreassian, and C. Perrin (2010), Are seemingly physically similar catchments truly hydrologically similar? *Water Resour. Res.*, *46*, W11558, doi:10.1029/2009WR008887.

Pilgrim, D. H. (1987), *Australian Rainfall and Runoff*, The Institution of Engineers, Australia.

Pilgrim, D. H., and I. Cordery (1993), Flood runoff, in *Handbook of Hydrology*, edited by D. R. Maidment, McGraw-Hill, New York, pp. 9.1–9.42.

Pui, A., A. Lall, and A. Sharma (2011), How does the interdecadal Pacific oscillation affect design floods in Australia?, *Water Resour. Res.*, *47*, W05554, doi:10.1029/2010WR009420.

Reichl, J. P. C., A. W. Western, N. R. McIntyre, and F. H. S. Chiew (2009), Optimisation of a similarity measure for estimating ungauged streamflow, *Water Resour. Res.*, *45*, W10423, doi:10.1029/2008WR007248.

Renard, B., D. Kavetski, G. Kuczera, and M. Thyer (2010), Understanding predictive uncertainty in hydrological modeling: The challenge of identifying input and structural errors, *Water Resour. Res.*, *46*, W05521, doi:10.1029/2009WR008328.

Rigby, E. H., and D. J. Bannigan (1996), The embedded design storm concept—A critical review, in *Hydrology and Water Resources Symposium 1996: Water and the Environment*, (online preprints of papers: *Natl. Conf. Publ. 96/05*), pp. 453–459, Institution of Engineers, Australia, Barton, Aust. Capital Terr.

Ropelewski, C., and M. S. Halpert (1987), Global and regional scale precipitation patterns associated with the El Nino/southern oscillation, *Mon. Weather Rev.*, *115*, 1606–1626.

Rosso, S., and T. Rigby (2006), The impact of embedded design storms within a catchment, in *30th Hydrology and Water Resources Symposium: Past, Present and Future*, Sandy Bay, Tasmania, Engineers Australia, Barton, Aust. Capital Terr., pp. 9–13 (online).

Salamon, P., and L. Feyen (2009), Assessing parameter, precipitation, and predictive uncertainty in a distributed hydrological model using sequential data assimilation with the particle filter, *J. Hydrol.*, *376*(3–4), 428–442.

Savitzky, A., and M. J. E. Golay (1964), Smoothing and differentiation of data by simplified least squares procedures, *Anal. Chem.*, *36*(8), 1627–1639.

Sharma, A., and R. Mehrotra (2010), Rainfall generation, in *Rainfall: State of the Science*, edited by F. Testik and M. Gebremichael, p. 32, AGU, Washington, DC.

Van den Dool, H. (2007), *Empirical Methods in Short-Term Climate Prediction*, 215 pp., Oxford University Press, Oxford.

Vaze, J., F. H. S. Chiew, J.-M. Perraud, N. R. Viney, D. A. Post, J. Teng, B. Wang, J. Lerat, and M. Goswami (2011), Rainfall-runoff modelling across southeast Australia: Datasets, models and results, *Aust. J. Water Resour.*, in press.

Westra, S., and S. A. Sisson (2011), Detection of non-stationarity in precipitation extremes using a max-stable process model, *J. Hydrol.*, *406*, 119–128.

Westra, S., I. Varley, P. Jordan, R. J. Nathan, A. Ladson, A. Sharma, and P. Hill (2010), Addressing climatic non-stationarity in the assessment of flood risk, *Aust. J. Water Resour.*, *14*(1), 1–16.

Westra, S., R. Mehrotra, A. Sharma, and R. Srikanthan (2012), Continuous rainfall simulation: 1—A regionalised sub-daily disaggregation approach, *Water Resour. Res.*, *48*, W01535, doi:10.1029/2011WR010489.

Wu, W., and R. E. Dickinson (2004), Time scales of layered soil moisture memory in the context of land atmosphere interaction, *J. Clim.*, *17*, 2752–2764.